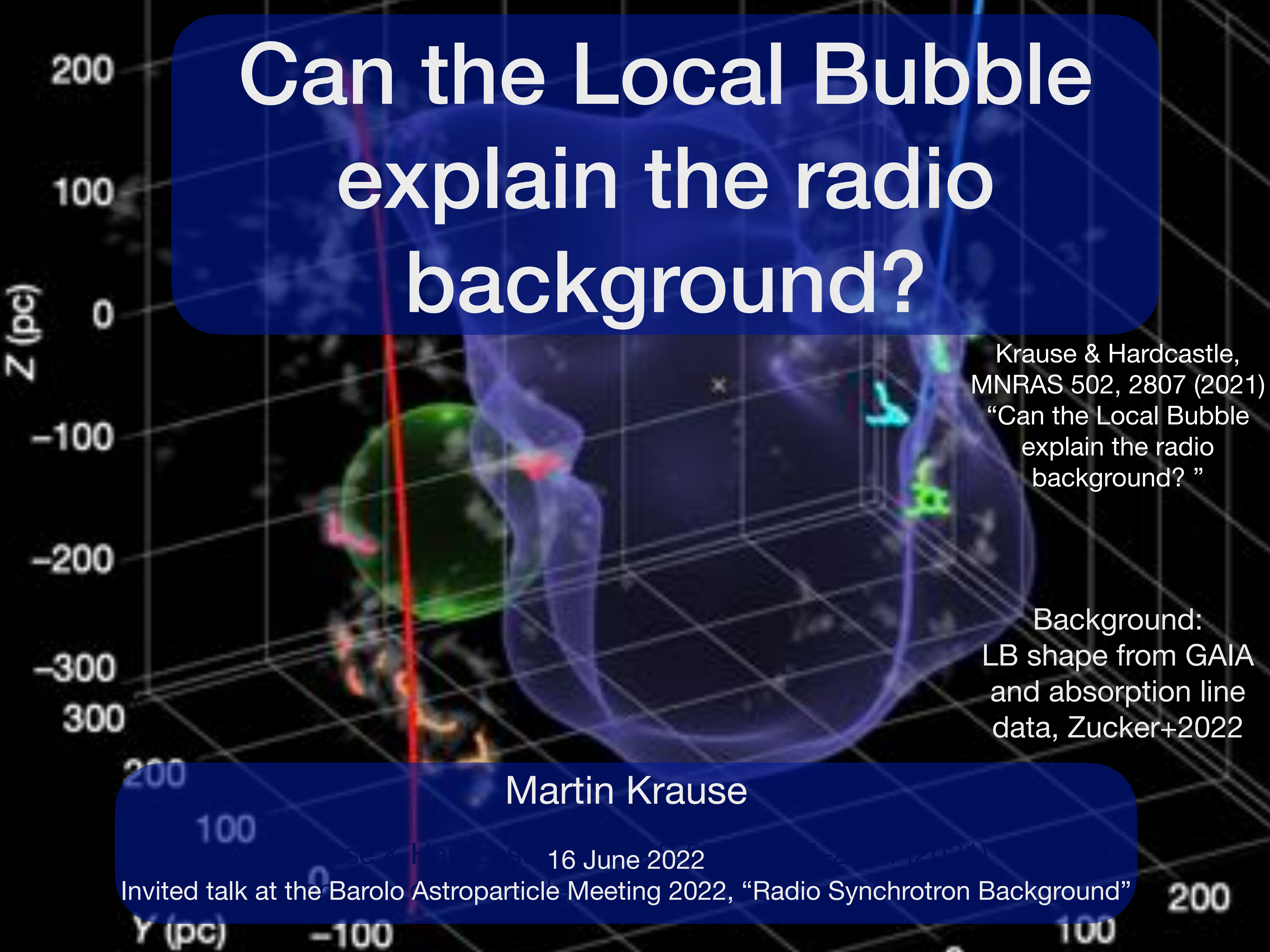

Can the Local Bubble explain the radio background?

Krause & Hardcastle, MNRAS 502, 2807 (2021) “Can the Local Bubble explain the radio background? ”

Background:
LB shape from GAIA and absorption line data, Zucker+2022

Martin Krause

16 June 2022

Invited talk at the Barolo Astroparticle Meeting 2022, “Radio Synchrotron Background”

Astronomical backgrounds

Big bang

Solar Wind / Local Bubble

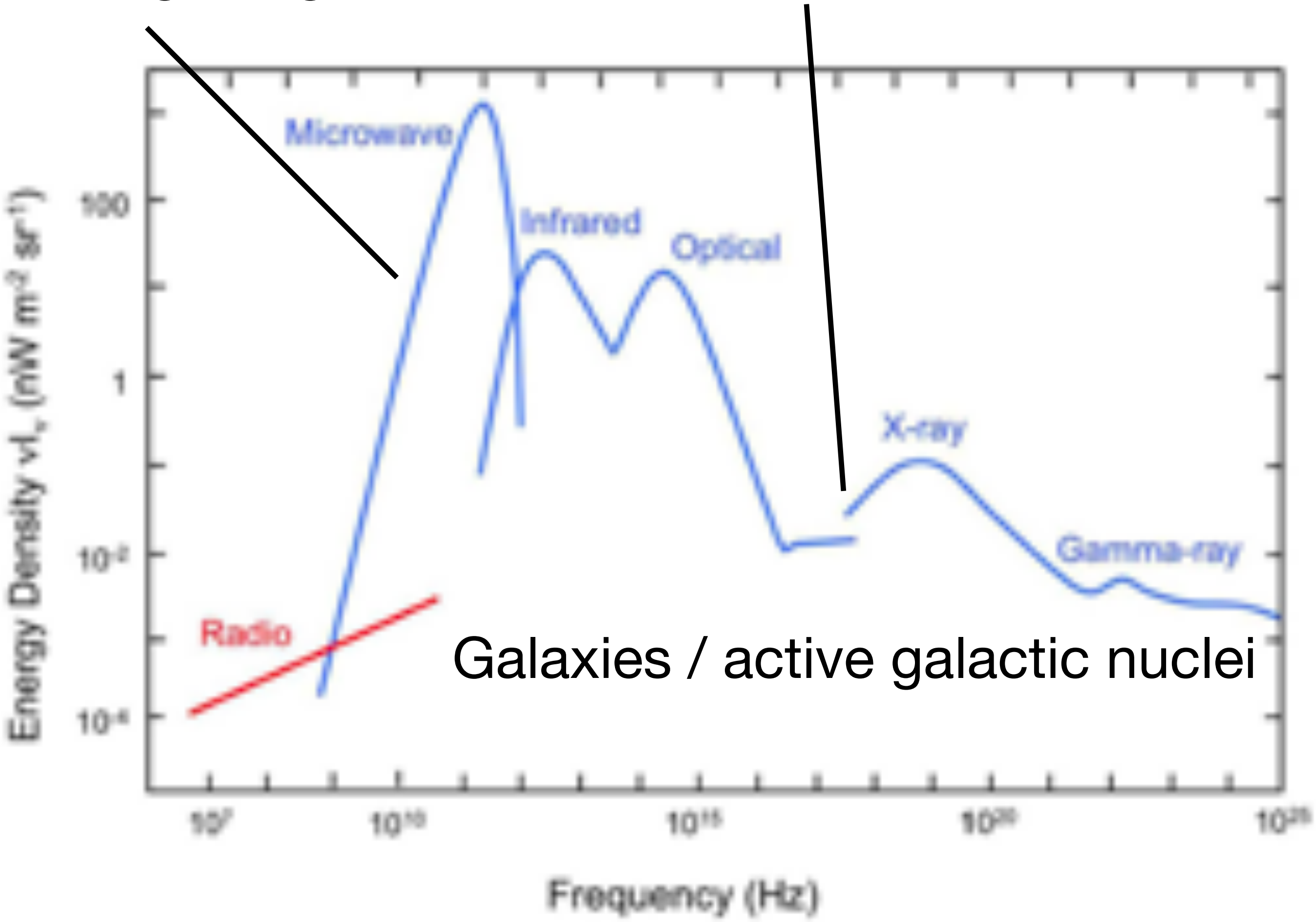

Galaxies / active galactic nuclei

Radio background: synchrotron spectrum

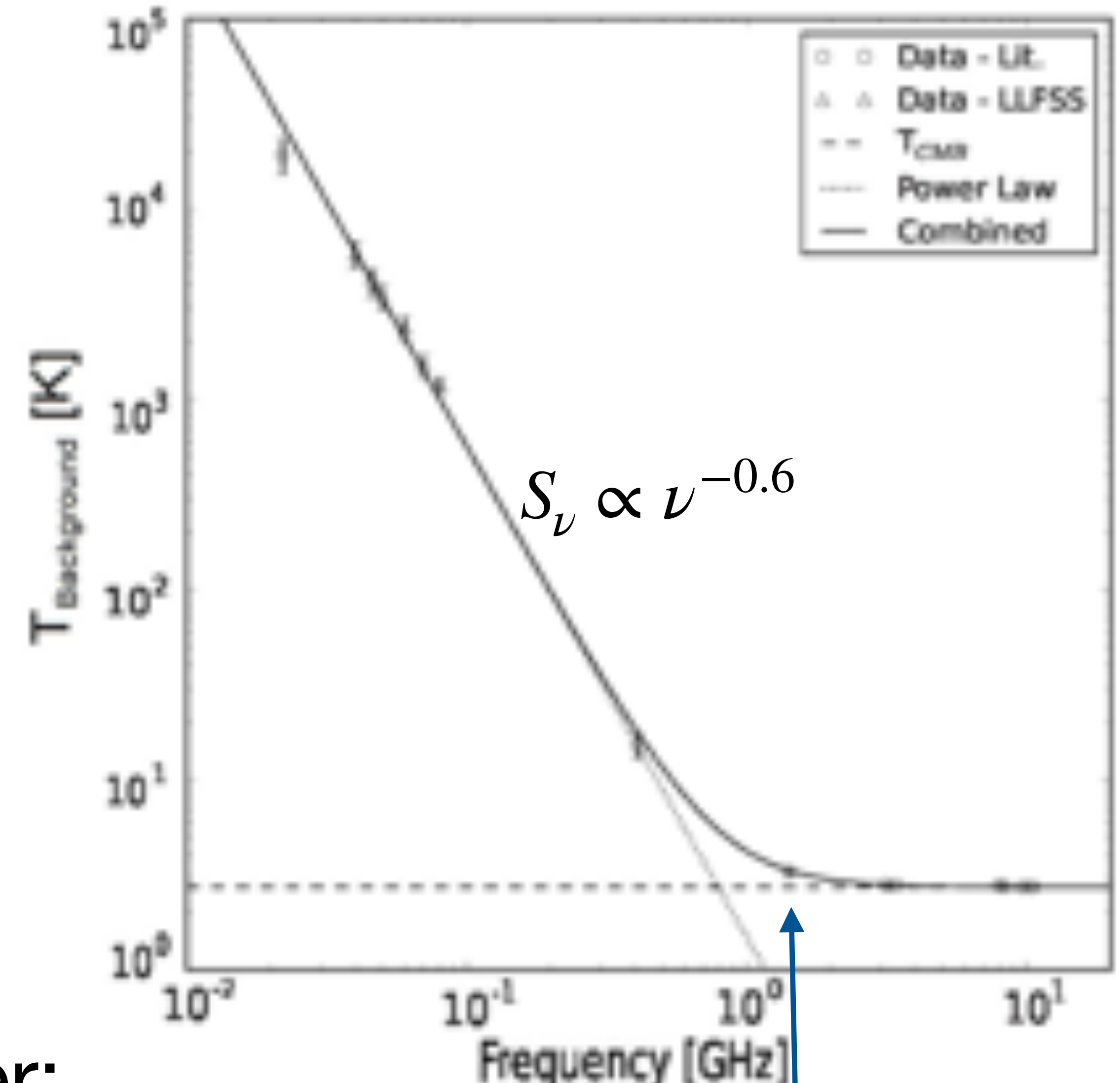

$S_\nu \propto \nu^{-0.6}$

- ARCADE 2 precision bolometer: 54±6 mK above CMB

Singal 2019

(1) Extrapolate from IC10 — Non-thermal Superbubble

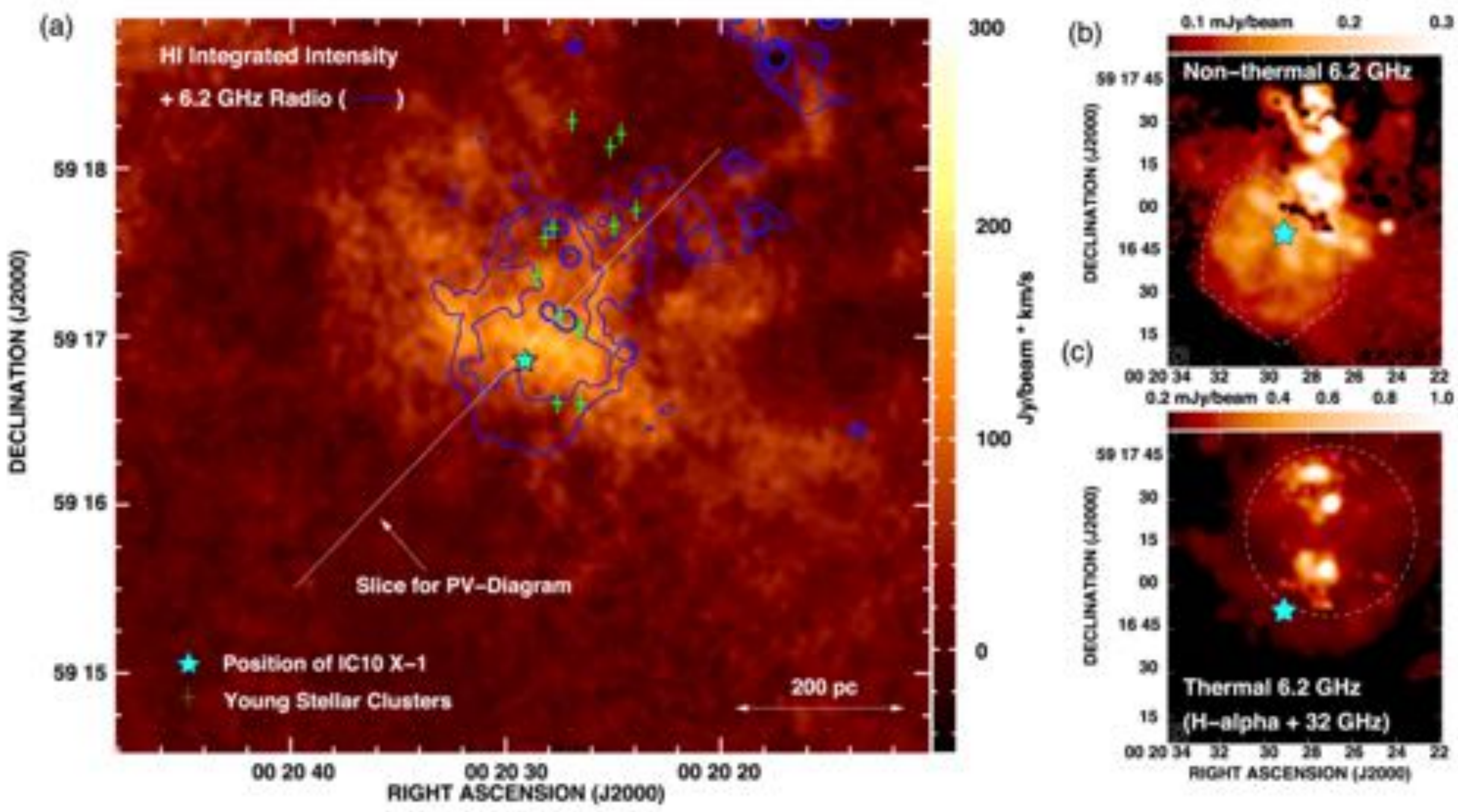

⇒ **Only non-thermal radio superbubble known. Few X-ray detections, see Lopez et al. 2020**

Heesen+2015

(1) Extrapolate from IC10 — Non-thermal Superbubble

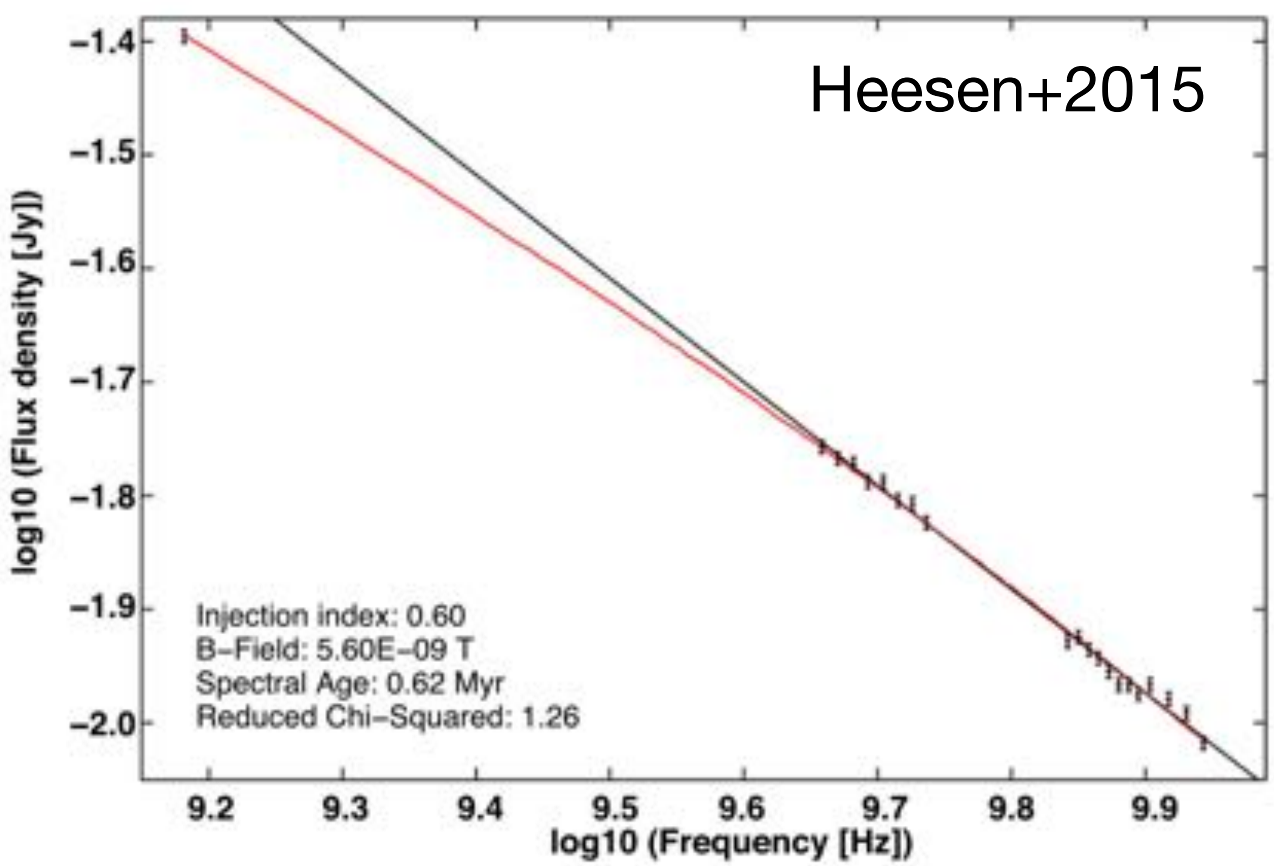

Figure 3. Non-thermal spectrum of the NSB between 1.5 and 8.8 GHz. The solid red line shows the Jaffe–Perola model fit to the data and the solid black line is a linear fit to data points >1.5 GHz.

- $S \propto \nu^{-0.6\pm0.1}$ (injection / low frequencies) ⇒Fits!
- ø = 200 pc ⇒Same as LB
- Scale down by $f_s = 0.1$ (suspect recent hypernova in IC 10), assume bubble radii of $100 f_{r10}$ pc and $100 f_{rLB}$ pc

$$\Rightarrow \quad T_\nu = 113 \left(\frac{f_s}{0.1}\right) f_{r10}^{-3}\, f_{rLB} \left(\frac{\nu}{3\,\mathrm{GHz}}\right)^{-2.6} \mathrm{mK}.$$

≈ 2 x radio background

Superbubbles can produce the right spectrum & flux!

Local Bubble

Extinction map:

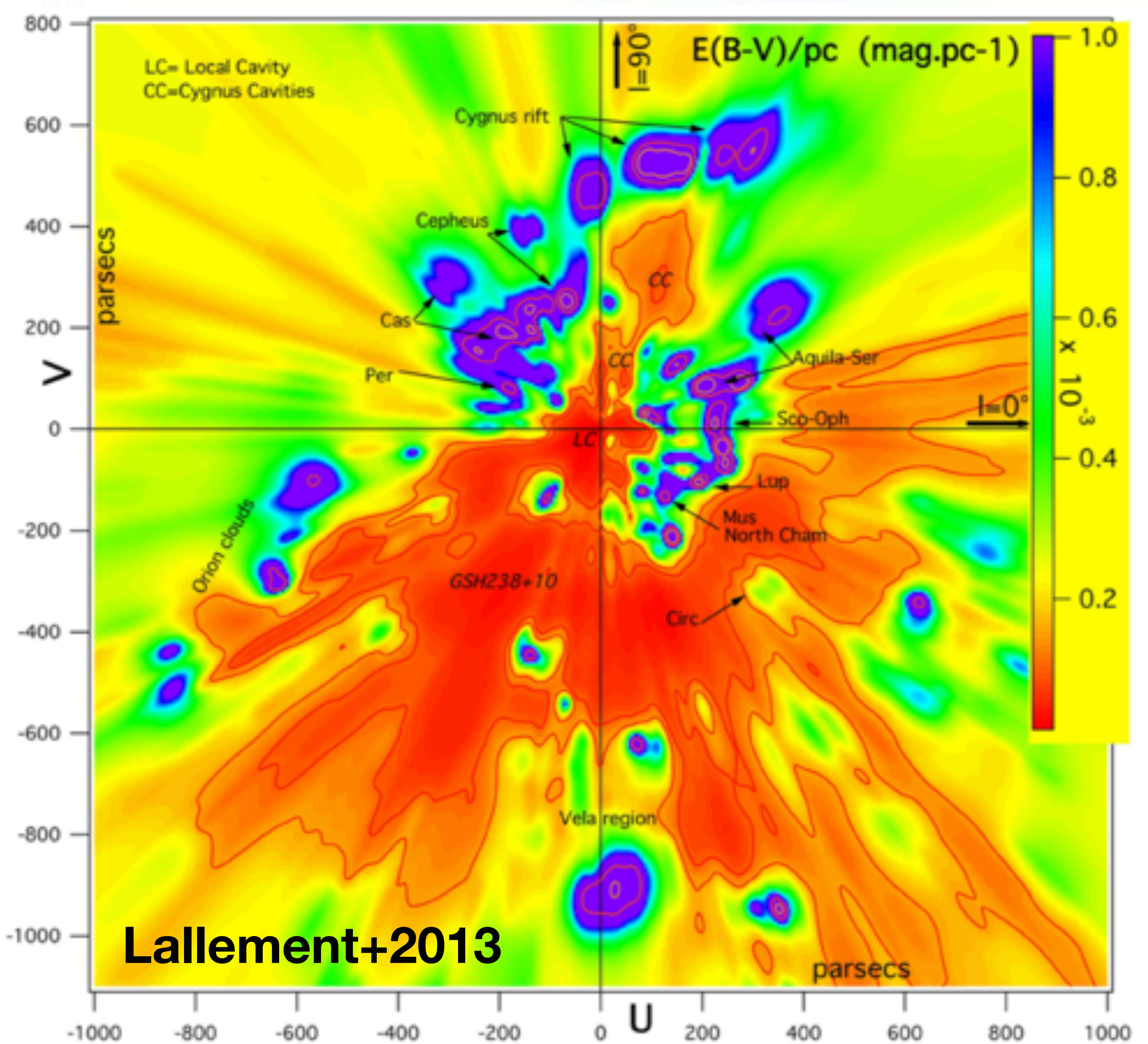

Zoom

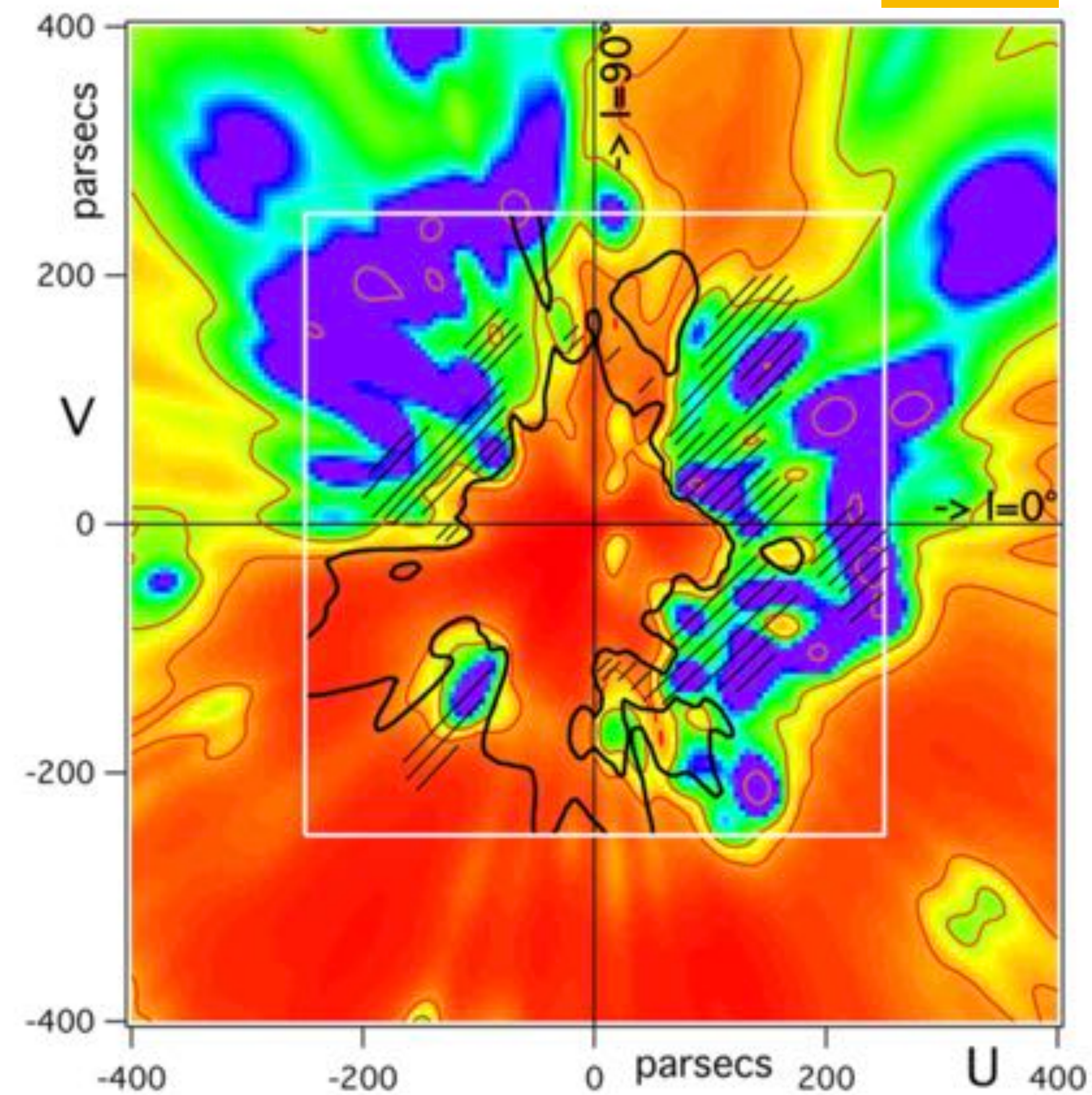

Also seen in X-rays, Snowden+1998, Snowden 2015

- Solar system is surrounded by a cavity, the local superbubble

Local Bubble

- Sun @ centre of ø ≈ 200 pc superbubble
- Formed by massive star winds and supernova explosions
- LB contributes to soft X-ray background
- LB threaded by magnetic fields
- Cosmic-ray electrons are directly measured near Earth
- ⇒LB is radio synchrotron emitter

Local Bubble:
magnetic field from pulsar polarisation

Xu & Han 2019

Table 2. Eight pulsars on the boundary of the Local Bubble.

Name	l (°)	b (°)	D (kpc)	DM (cm^{-3} pc)	RM rad m^{-2}	$\langle B_{\|\|} \rangle$ (μG)
J1057–5226	285.984	6.649	0.09	29.69	47.2 ± 0.8	1.96 ± 0.03
J0711–6830	279.531	−23.280	0.11	18.41	23.9 ± 0.4	1.60 ± 0.03
J0749–68	281.031	−20.014	0.11	26.00	-23.0 ± 2.0	-1.09 ± 0.09
J0924–5814	278.395	−5.595	0.11	57.40	-45.0 ± 1.0	-0.97 ± 0.02
J1016–5345	281.201	2.451	0.12	66.80	-21.0 ± 4.0	-0.39 ± 0.07
J1000–5149	278.107	2.603	0.13	72.80	46.0 ± 9.0	0.78 ± 0.15
J0536–7543	287.162	−30.821	0.14	18.58	23.8 ± 0.9	1.58 ± 0.06
J1105–43	283.511	14.886	0.14	45.50	17.0 ± 1.0	0.46 ± 0.03

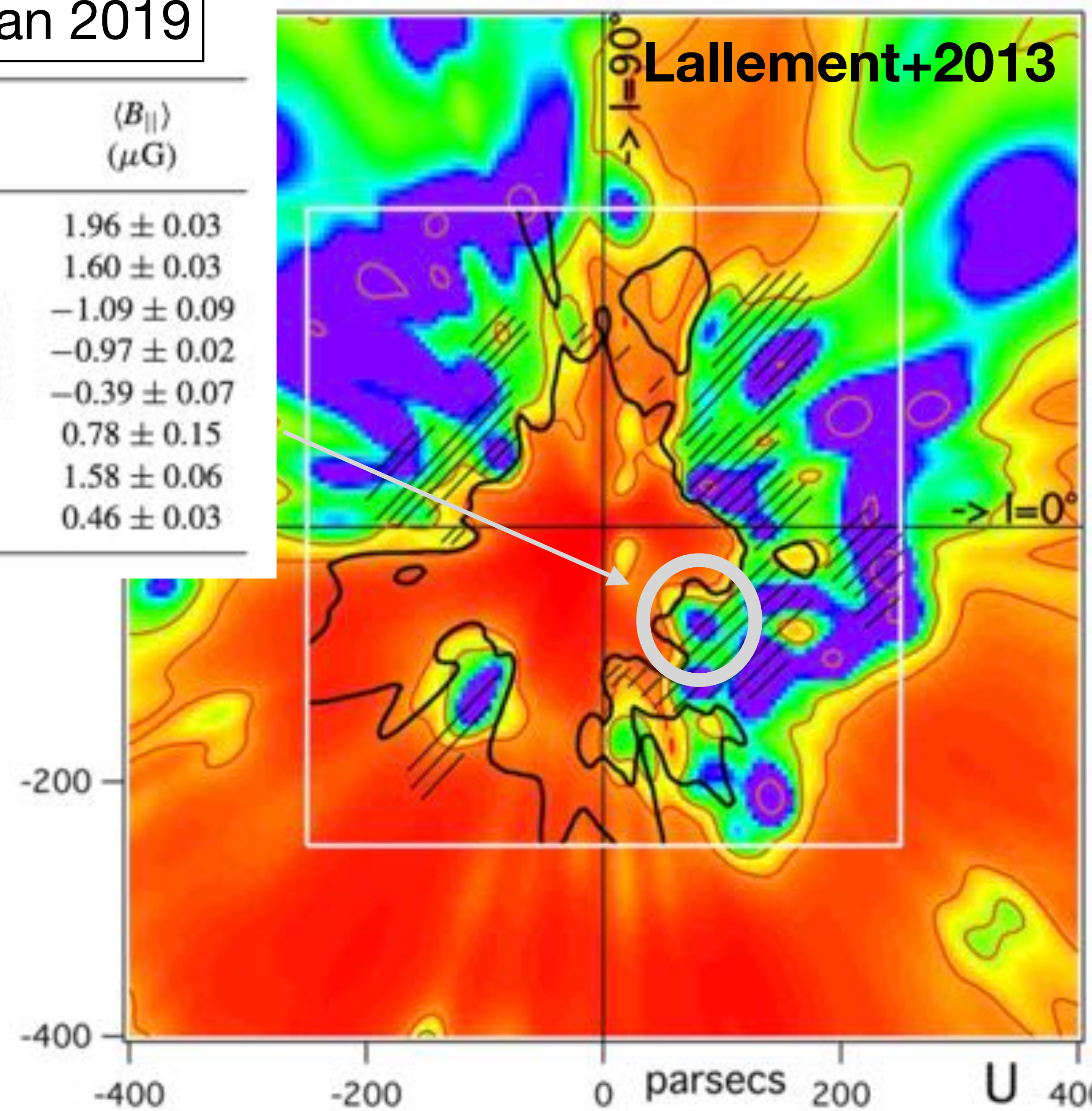

- Dispersion of radio pulses ⇒ thermal electron column $N_e \approx 10^{24}\,\mathrm{cm}^{-2}$, likely from bubble wall
- Faraday rotation:
- clouds: $RM < 4\,\mathrm{rad\,m^{-2}} \left(\frac{n_e}{n_{e,wc}}\right)\left(\frac{B_{los}}{0.5\,\mathrm{nT}}\right) f_{wcp}$
- hot intercloud gas ($T_X \approx 0.1$ keV, $n_{e,X} \approx 5 \times 10^3\ m^{-3}$, Snowden et al 2014):

$$RM < 38\,\mathrm{rad\,m^{-2}} \left(\frac{n_e}{n_{e,X}}\right)\left(\frac{B_{los}}{10\,\mathrm{nT}}\right) f_{rLB}.$$

⇒ B ≤ 100 μG (10nT)

3D hydrodynamics simulations

Corresponds to typical few 1000 M_{sun} cluster (compare Kroupa 2012), e.g. Sco-Cen

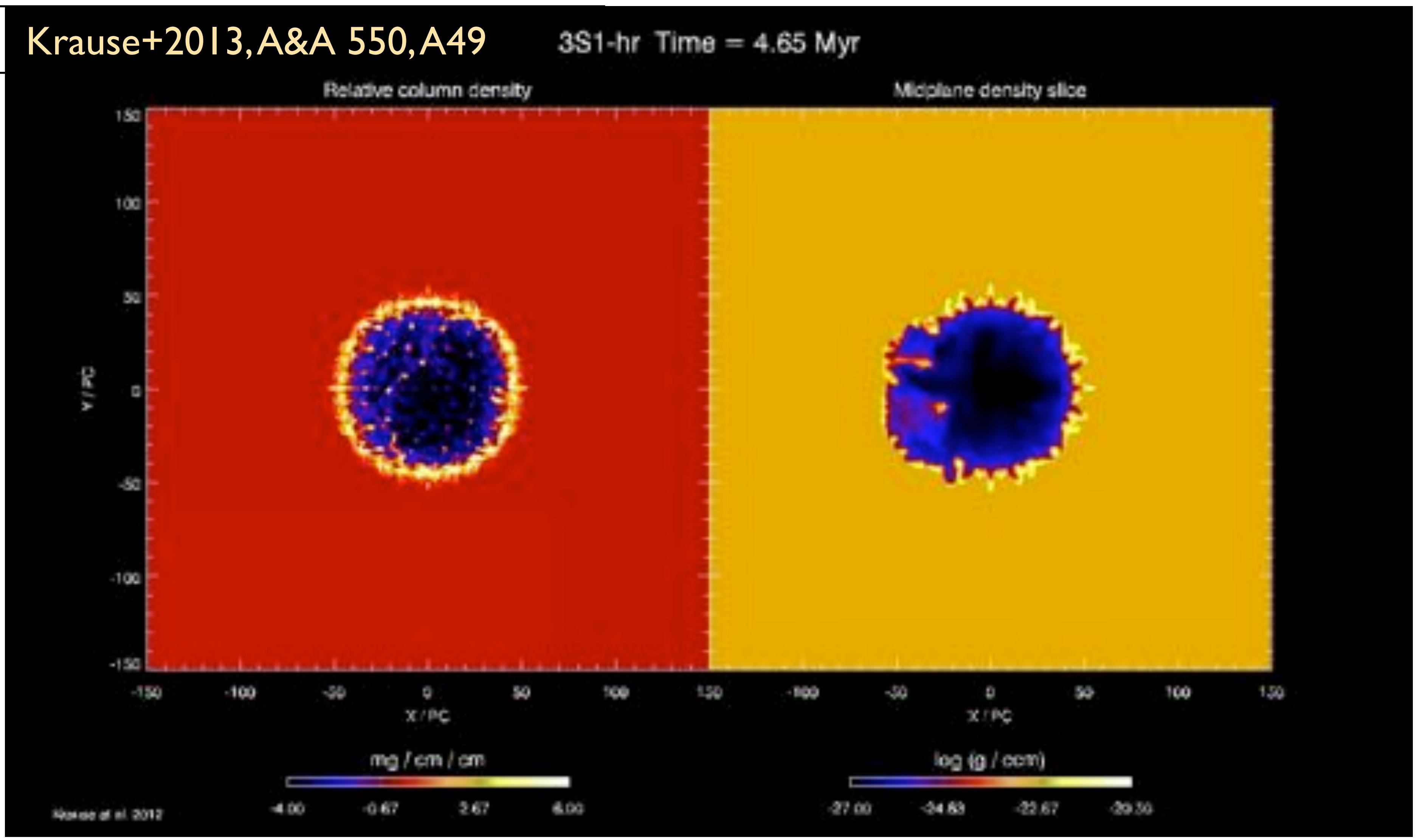

At SN #1: ø ≈ 80 pc (10 cm^{-3} ambient), secondary O-star winds compressed to filaments

- 3 stars, 25, 32, 60 M_{sun}, full evolution inc. SN
- bubble merging
- shell clumping: Vishniac instability (decelerating phases)
- mixing layer: Rayleigh-Taylor instability (accelerating phases)

3pc around Sun

- partially ionised clouds
- Obs: absorption of star light, Solar Wind, Energetic Neutral Atoms interactions
- $N_{HI} \approx 10^{18}$ cm^{-2},
  ø ≈ 1-10 pc
  B ≈ 0.3 nT
- LB filled with such “warm clouds” / filaments

The Astrophysical Journal, 886:41 (19pp), 2019 November 20 Linsky, Redfield, & Tilipman

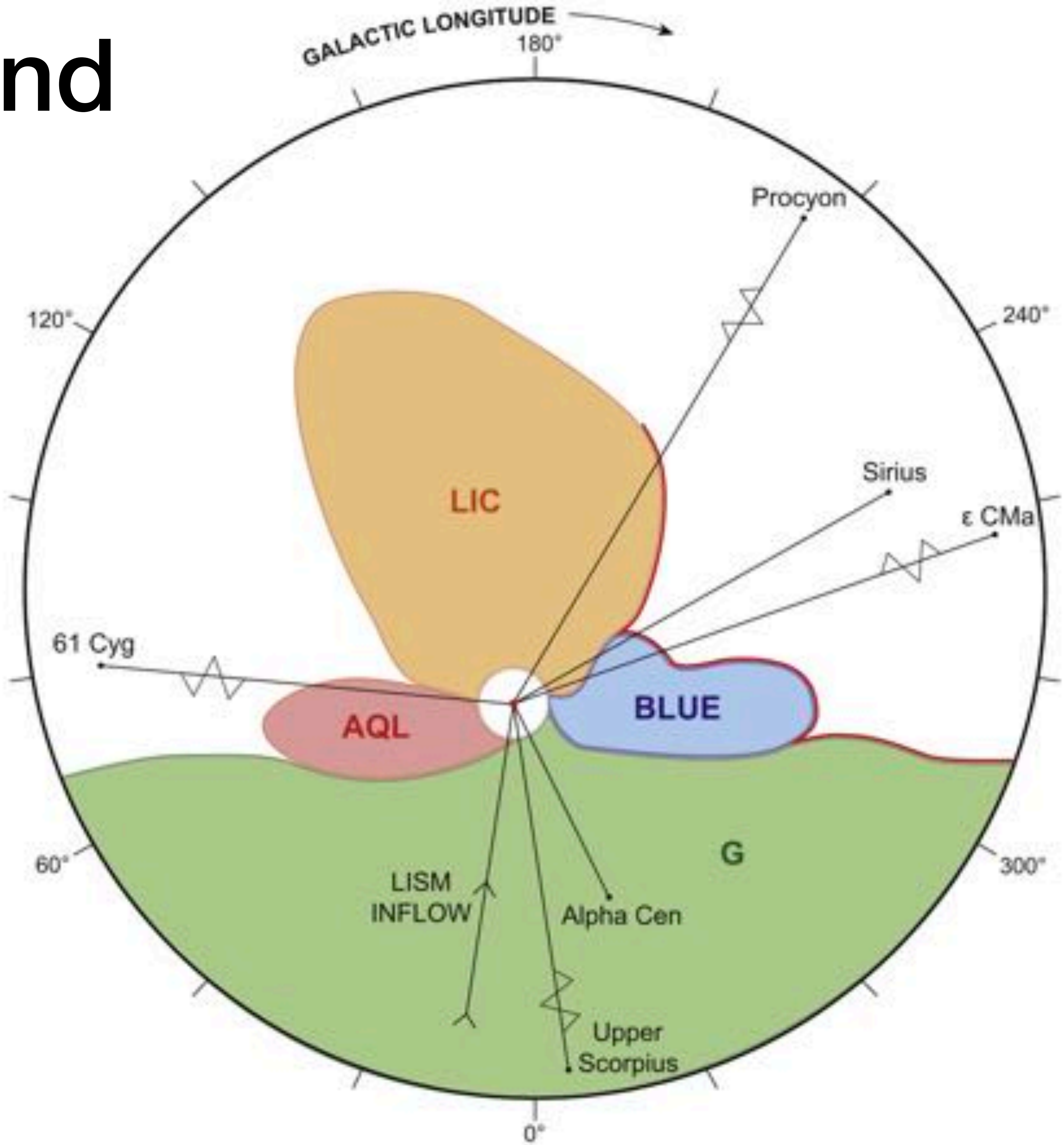

Figure 11. The local ISM region within 3 pc of the Sun as viewed from the north Galactic pole, showing the location of the four partially ionized clouds that are in contact with the outer heliosphere. Not shown are other clouds lying outside the four clouds. Shown are the Sun (point), an exaggerated representation of the heliopause (circle around the Sun) and the LIC, G, Aql, and Blue clouds. Lines of sight projected onto the Galactic equator are shown for five stars. Red shading shows the Strömgren shells produced by EUV radiation from ε CMa. Also shown are the direction of inflowing interstellar gas as seen from the Sun and the direction to the Upper Scorpius region of the Scorpius–Centaurus Association, where the most recent supernovae likely occurred.

Last supernova in Local Bubble?

⇒Deposition of radioactive ^{60} Fe in Earth crust

- ^{60}Fe: $t_{1/2}$ = 2.6 Myr
- Only produced in supernovae
- peak 2-3 and 7-8 Myr ago: recent SN in Local Bubble

⇒ Last supernova in Local Bubble: 2-3 Myr ago

crossing time / shock wave: ≈ 0.2 Myr

⇒ turbulence from this event has largely decayed now

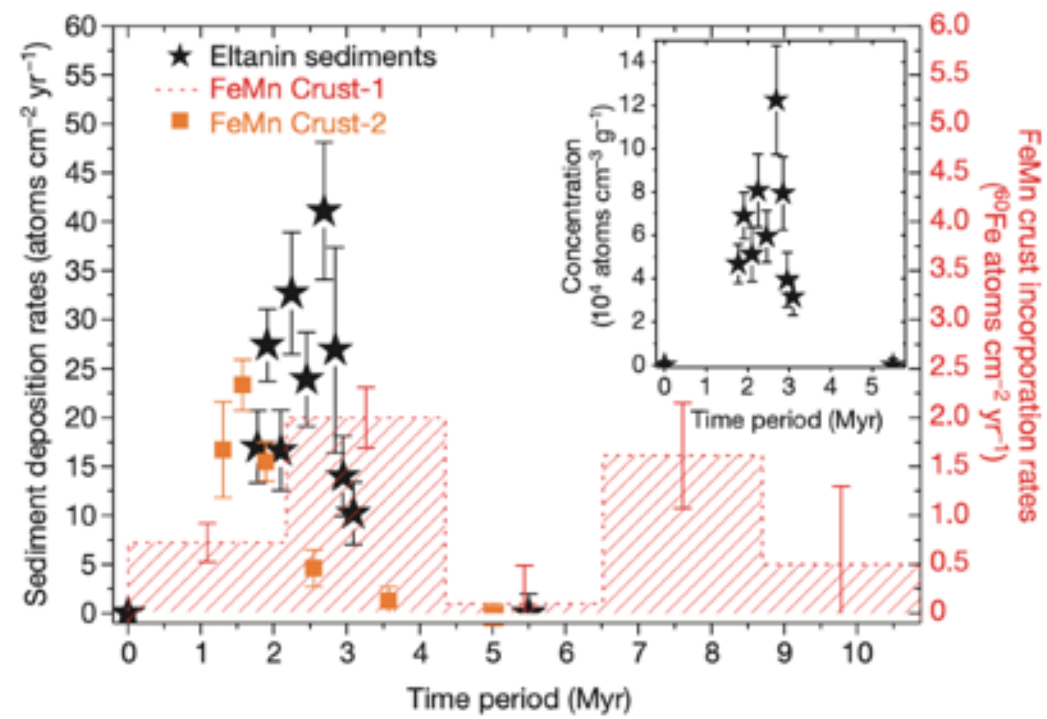

Figure 1 | Deposition rates for sediment (150-kyr averaged data) and incorporation rates for two crust samples. ^{60}Fe concentrations (^{60}Fe per gram) for the sediment are given in the inset; they were on average 6.7×10^4 atoms per gram between 1.7 Myr and 3.2 Myr, but 260×10^4 atoms per gram of crust and 95×10^4 atoms per gram of nodule, reflecting the difference in growth rate and incorporation efficiency (see Supplementary Information). The error bars (1σ Poisson statistics) include all uncertainties and scale with decay correction, so that uncertainties and upper limits become larger for older samples. The absolute ages for the sediment samples have an uncertainty of 0.1 Myr, except for the 5.5-Myr-old sediments, which have an uncertainty of about 1 Myr. The age of Crust-1 has an uncertainty of 0.3 Myr and the age of Crust-2 has an uncertainty of 0.5 Myr.

Magnetic geometry from starlight polarisation

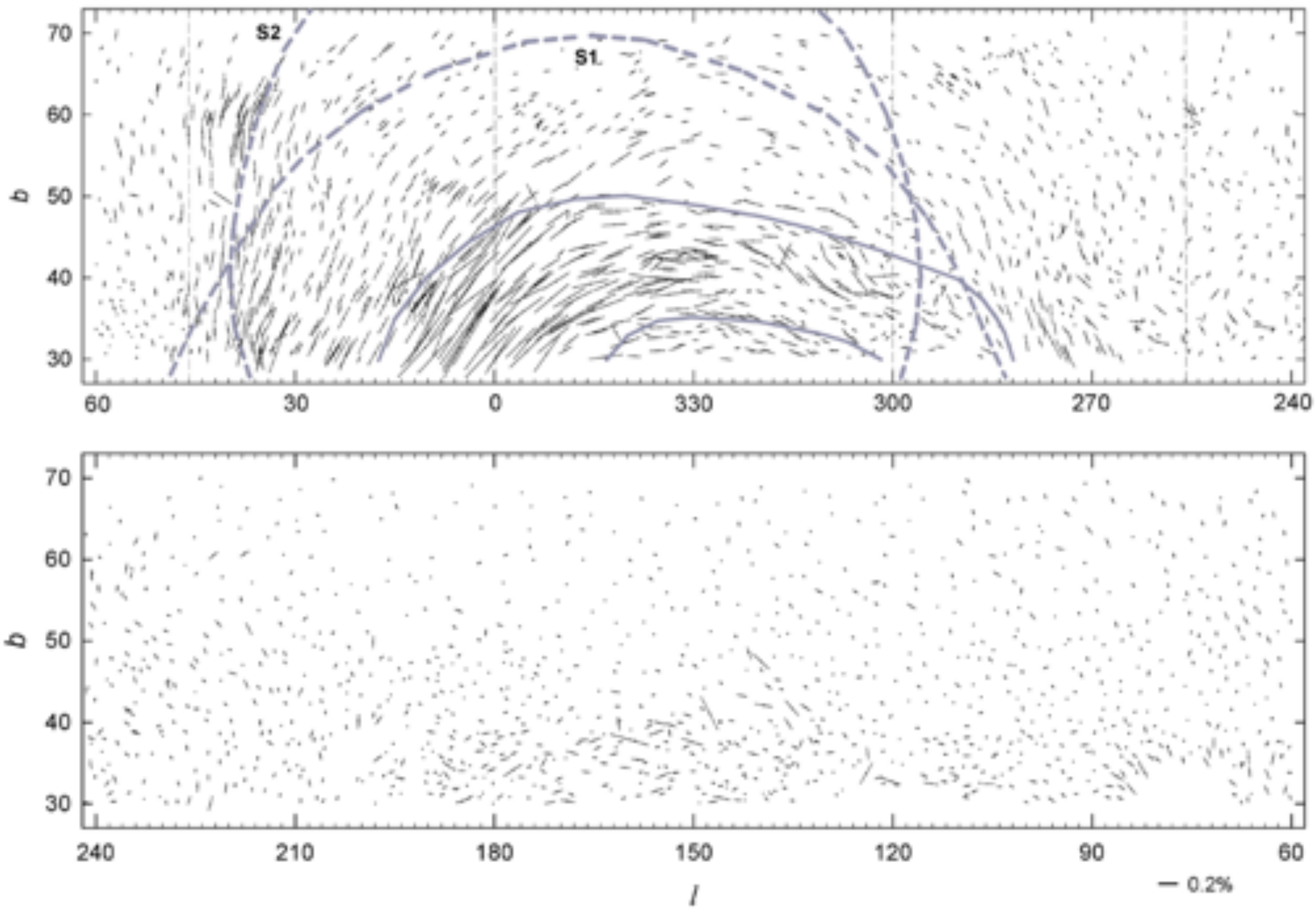

Berdyugin et al. 2014

- D≈ 100-500 pc
- large coherent polarisation where bubble wall closest
- turbulent field, coherence length <≈ 40 pc otherwise
- consistent with decaying turbulence after last SN, ca. 2-3 Myr ago (^{60}Fe ocean sediments, Wallner et al. 2016)

Magnetic field strength from turbulence theory

- Inverse cascade if magnetic energy density dominates (e.g., Brandenburg et al. 2015)
- Thermal energy density (Snowden et al. 2014): $2 \times 10^{-13} \left(\frac{n_\mathrm{e}}{5 \times 10^{-3}\,\mathrm{m}^3}\right)\left(\frac{T}{0.1\,\mathrm{keV}}\right)$ J/m³
- Magnetic energy density: $2 \times 10^{-13} \left(\frac{B}{0.6\,\mathrm{nT}}\right)^2$ J/m³
- $\Rightarrow$ for $B > 0.6$ nT : tension / lack of large-scale coherence in starlight polarisation! Hence, B limited to:
  - 100 μG (10 nT) by pulsar rotation measures
  - 6 μG (0.6 nT) for equipartition with thermal X-ray gas
  - 2 μG (0.2 nT) for equipartition with non-thermal electrons (below)

Non-thermal electrons: direct measurements

- direct measurements by Voyager 1 (left Heliosphere) & AMS on International Space Station
- Connect with CR propagation model through Heliosphere

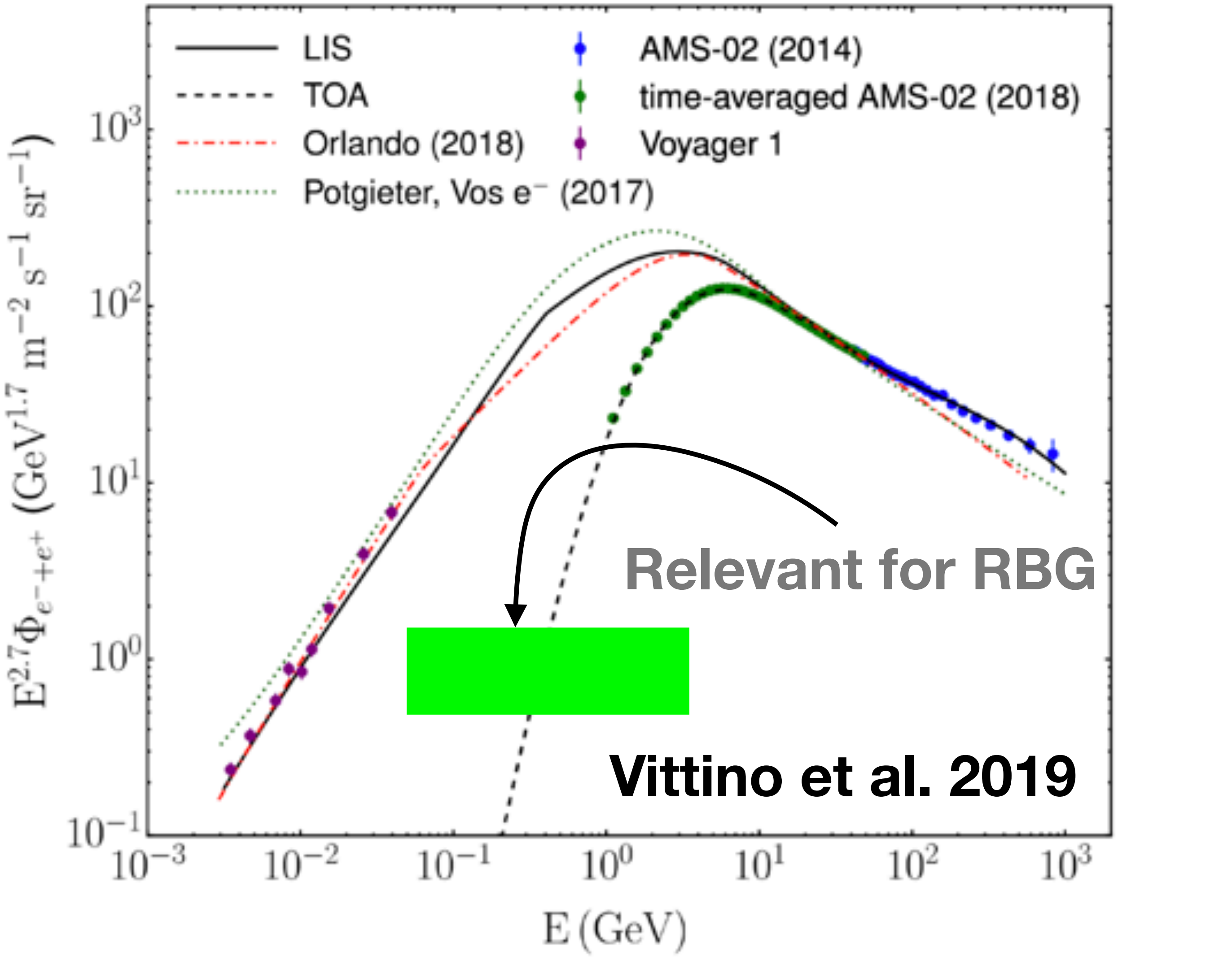

Our emission model

- 256^3 cube with turbulent random field , e.g. Tribble (1991) and Murgia et al. (2004)
- magnetic vector potential drawn from Rayleigh distribution
- use Kolmogorov power spectrum,
  vary cutoff scale for large modes (decaying turbulence)
- uniformly filled with non-thermal electrons with locally measured properties
- calculate synchrotron emission and polarisation with standard formula

Results: sky maps

SN just happened
⇒ large fluctuations

SN some time ago, turbulence decaying
⇒ smaller fluctuations, low polarisation
⇒ consistent with radio background

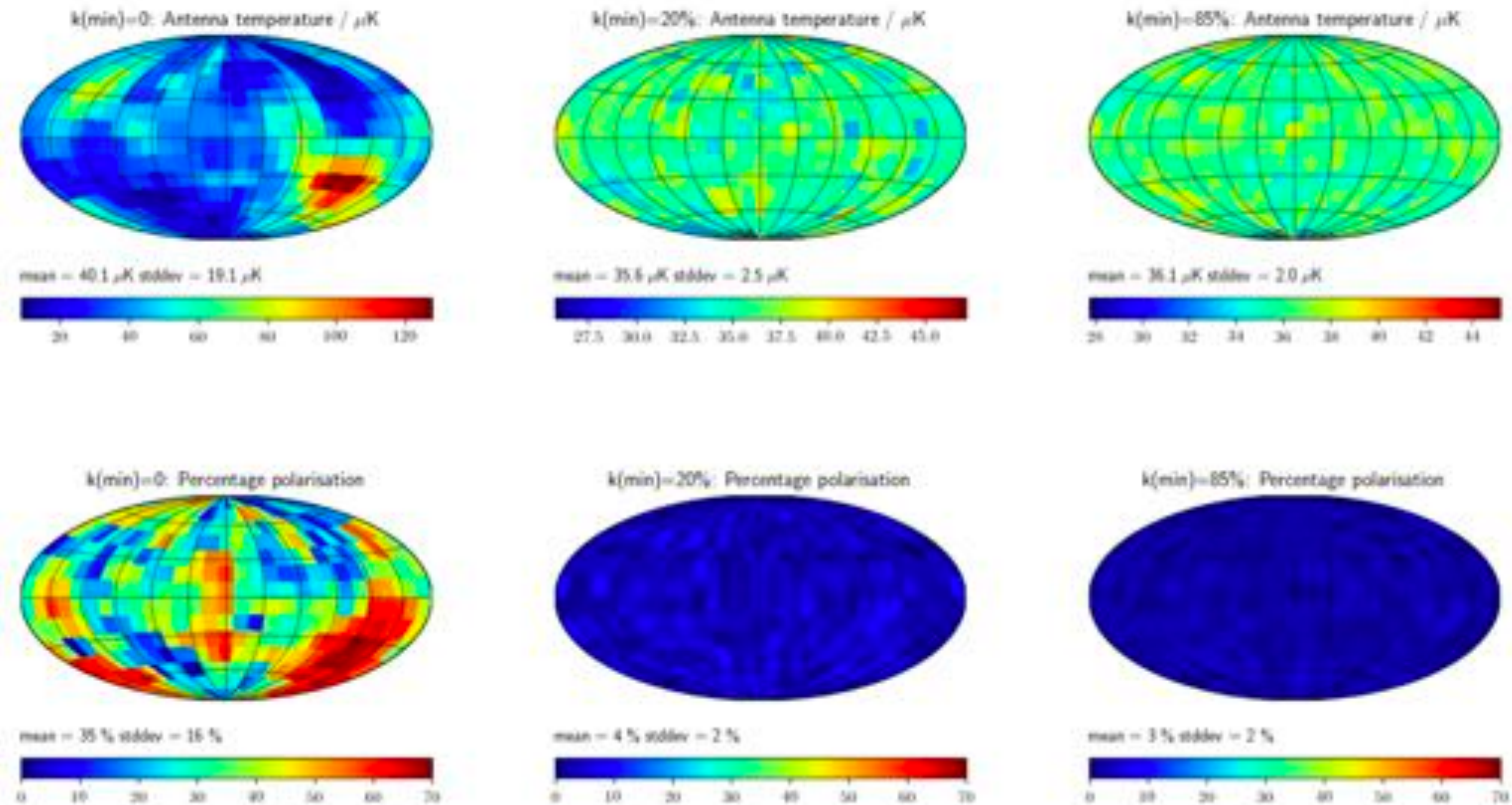

Synthetic radio sky with a mean magnetic field of 1.6nT at 3.3GHz, resolution is12° matching that of the ARCADE 2 radiometer.

Results: spectrum

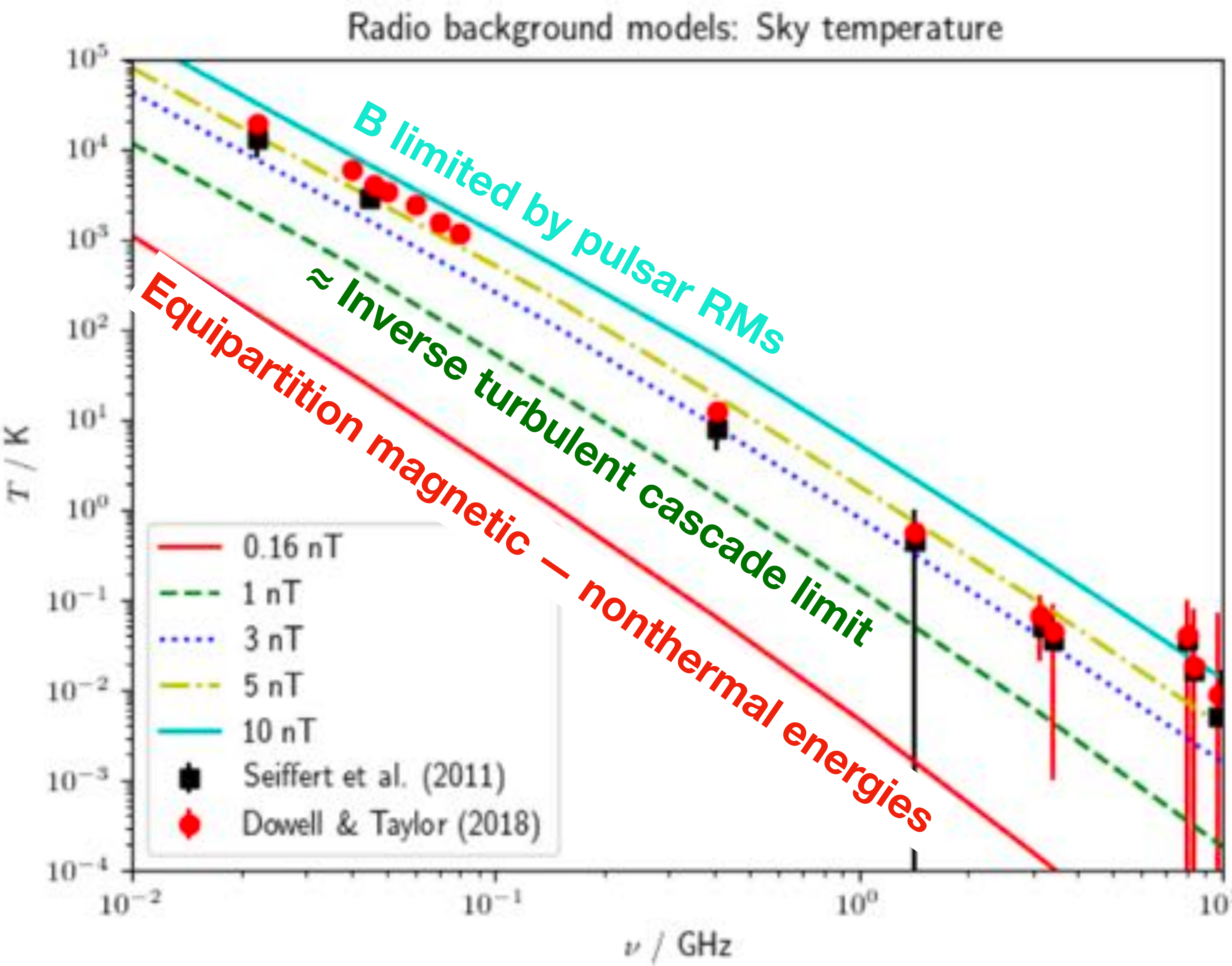

- Spectrum fits very well
- Can explain up to 100% of RBG if B limited only by pulsar RMs
- Can explain 1-few% of RBG if want to avoid dominant mag. field, i.e. inverse cascade (likely)

Conclusions

- LB properties well constrained by observations
- Good measurements of magnetic field & rel. electrons
- LB probably contributes 1 to a few % to radio background
- 20-25%: discrete extragalactic sources
- i.e. $\gtrapprox$ 70% of radio background currently not well understood

Conclusions

- LB probably contributes 1- a few % to radio background (why? very different from IC 10 NTSB)
- 20-25%: discrete extragalactic sources
- i.e. >≈ 70% of radio background currently not well understood
- new sources / populations are hypothesised: dark-matter annihilation, population-III supernovae, dark stars, quark nuggets, …
- my personal next guess: giant bubbles from radio-AGN in small galaxies …

Radio AGN bubbles from small galaxies fill ≈ 30% of Universe @ z=0 (Furlanetto & Loeb, 2001)

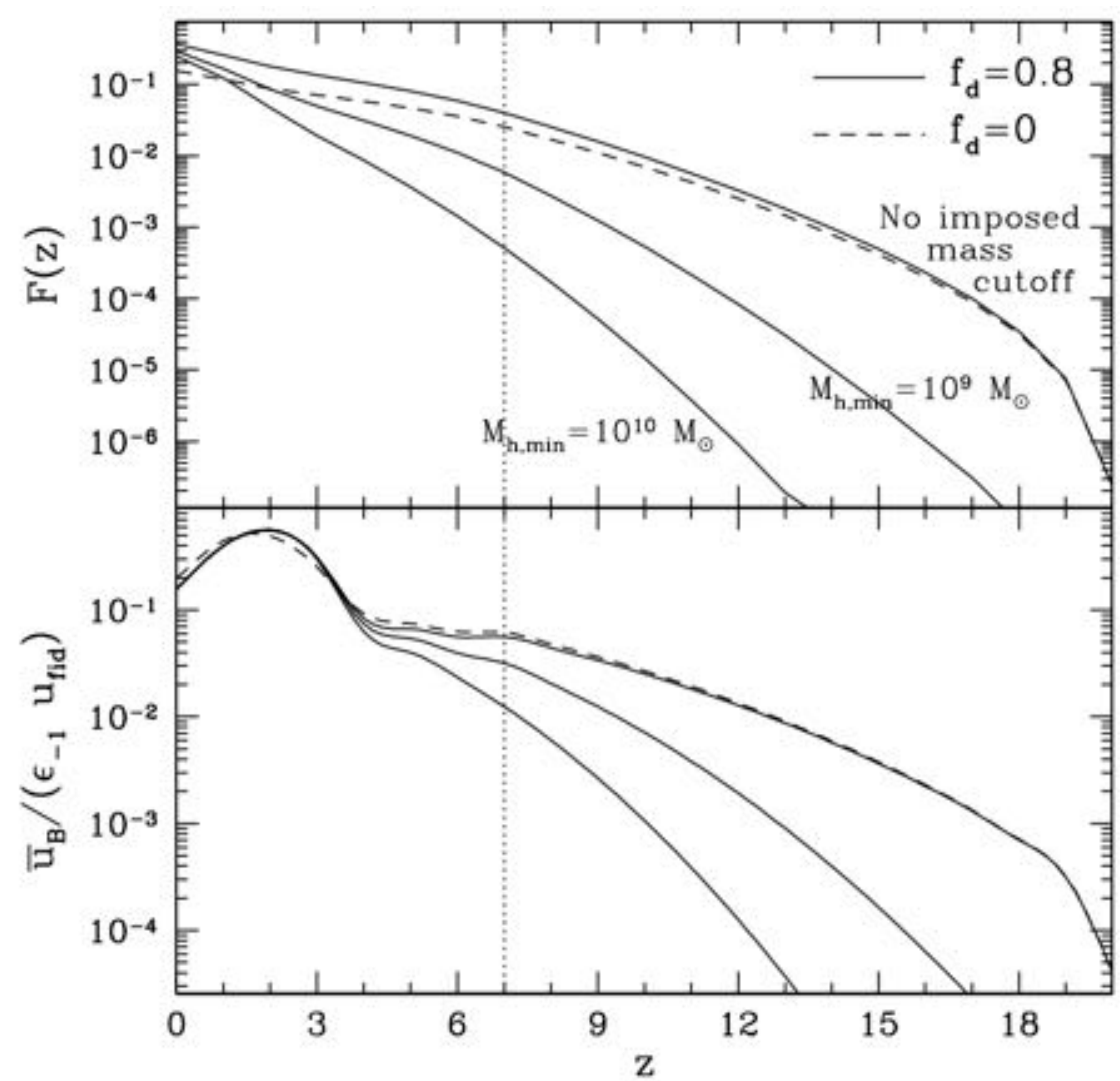

Part of Milky Way halo?

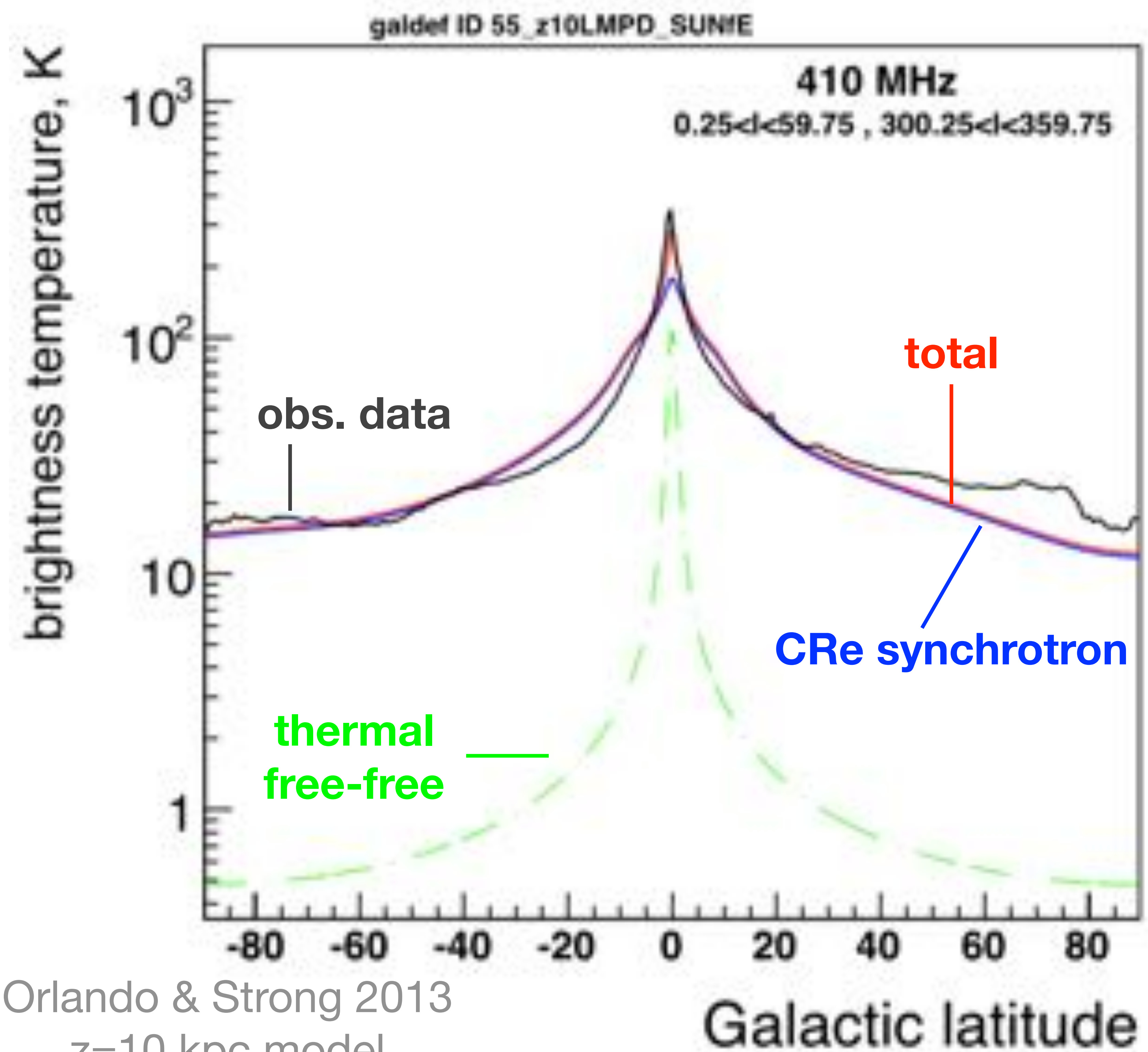

Orlando & Strong 2013
z=10 kpc model

- Significant residual radio continuum emission even at b = 90 deg
- Galactic model (galprop CRe prop.) requires 10 kpc scale height of cosmic ray electrons
- ⇒ unrealistic

Radio halos in external galaxies

Stein et al. 2019:

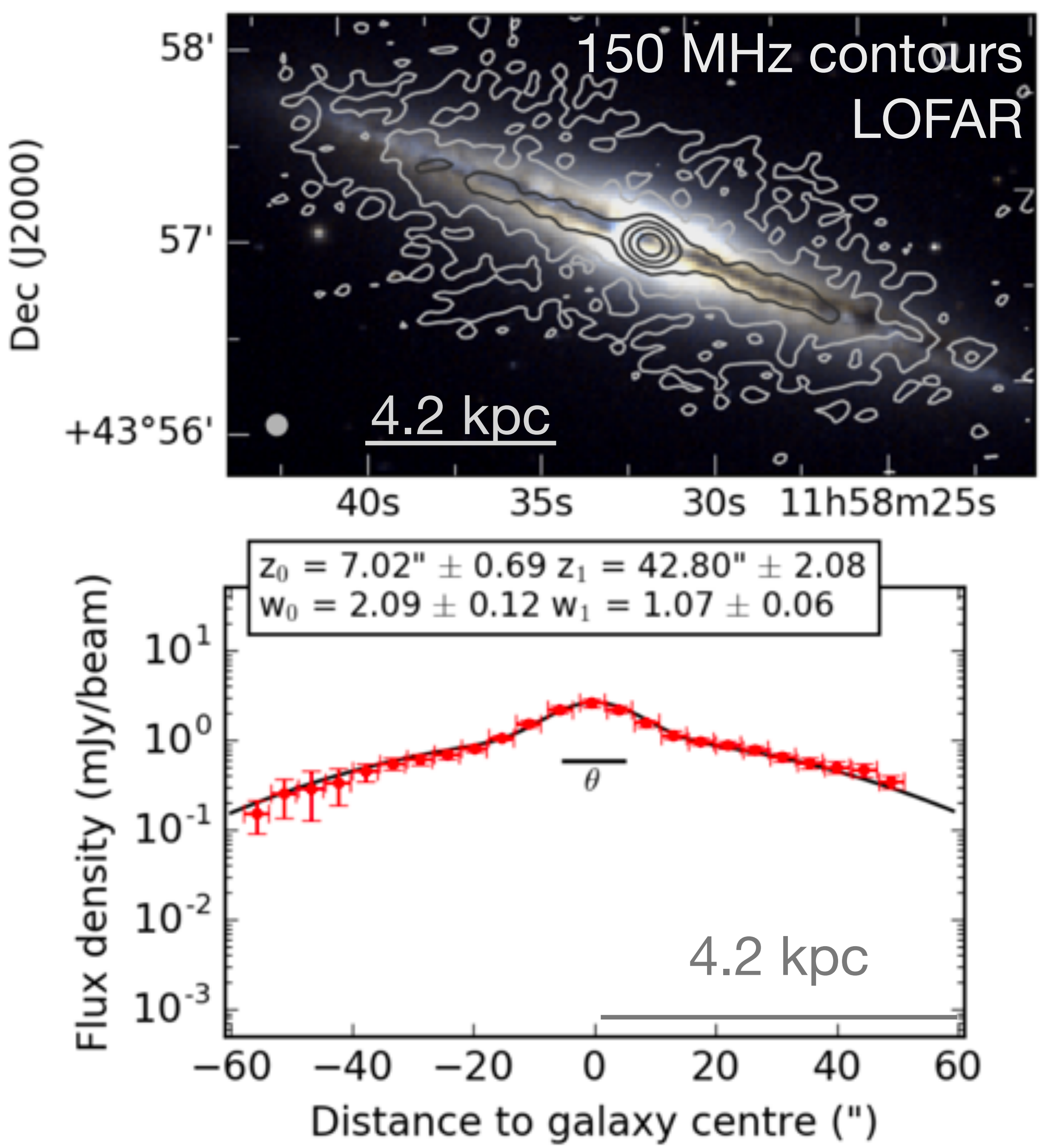

- Example: NGC 4013: scale height = 3 kpc @ 150 MHz
- Smaller at higher frequency
- This is a already a comparatively prominent halo

Discrete extragalactic sources

- @144 MHz: ≈ 25% (Hardcastle et al. 2021)
- @1.4GHz: ≈ 20% (Condon et al., 2012)

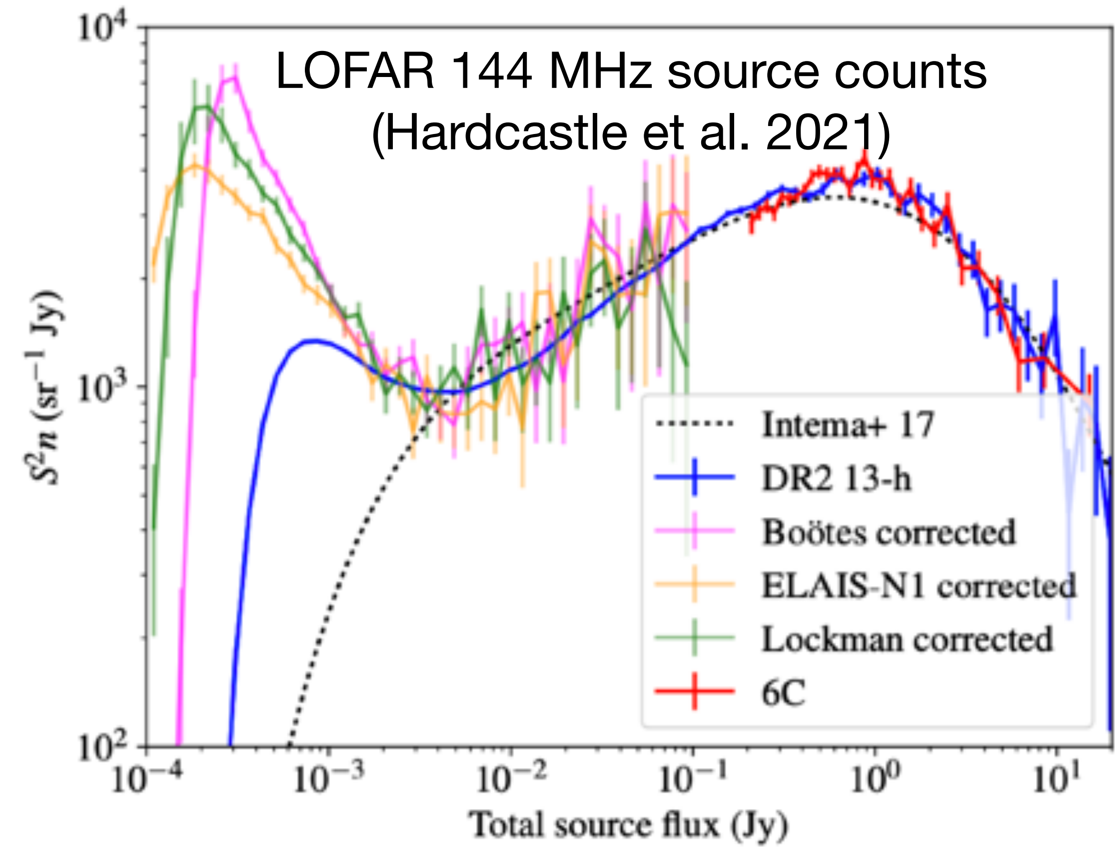

- New hypothetical sources would be required that are *faint* and *numerous*